Freezing kinetics in overcompressed water

Marina Bastea,* Sorin Bastea, John E. Reaugh, and David B. Reisman
Lawrence Livermore National Laboratory, P.O. Box 808, Livermore, California 94550, USA
(Received 3 October 2006; published 14 May 2007)

We report high-pressure dynamic compression experiments of liquid water along a quasiadiabatic path leading to the ice-VII region of the phase diagram. We observe dynamic features resembling van der Waals loops and find that liquid water is compacted to a metastable state close to the ice density before the onset of crystallization. By analyzing the characteristic kinetic time scale involved we estimate the nucleation barrier and conclude that liquid water has been compressed to a high-pressure state close to its thermodynamic stability limit.

DOI: 10.1103/PhysRevB.75.172104 PACS number(s): 64.70.Dv, 62.50.+p, 64.60.Qb

The transformation of water into ice is among the most common first-order phase transitions occurring in nature, but it is far from being an ordinary one.[1] Water has unusual physical properties both as a liquid and as a solid due largely to hydrogen bonding effects, which also play a major role in determining the characteristics of its freezing kinetics. Most studies aimed at understanding this process have been focused on the water-ice transformation kinetics following a temperature quench at low pressures.[2–4] Ice is known to have numerous crystalline phases, most of them occurring under high-pressure conditions.[5] A single phase though, ice VII, occupies a large region of the phase diagram at pressures above 2 GPa and has been known as the dominant high-pressure phase.[6,7] Ice VII is believed for example, to play an important role in the physics of outer planetary bodies,[8] and its detailed properties are still a matter of some debate.[9–11] In the present paper we probe the liquid-water–crystalline-ice phase transformation kinetics by magnetically driven fast compression along a quasiadiabatic path leading to the ice-VII region of the phase diagram.

Ultrapure water samples were encapsulated in the anode of the Z-accelerator[12] in 12-mm-diameter disk-shaped counterbores (see Fig. 1) using various transparent windows. The floor thickness of the aluminum (Al) anode containing the water samples was 1 mm, specifically designed to delay magnetic field penetration until after the pressure in the sample reaches its maximum value. Since water is a very corrosive medium even at ambient conditions, a layer of platinum (Pt) was deposited over most of the surfaces in contact with it to preclude oxidation—i.e., over the entire Al anode counterbore and $\simeq$80% of the back of the reflective coating on the window (a small opening in the coating was left on the periphery of the window for *in situ* metrology and visual inspection). A comprehensive chemical analysis of water specimens exposed to typical contaminants for approximately 100 times longer than in the actual experiments was carried out by gas chromatography and mass spectrometry. Negligible amounts of polymeric compounds (<10 parts per 10^9) were identified and related primarily to the o-ring sealing the water cavity between the window and Al anode. The thickness (300–500 μm) and planarity of the samples were measured *in situ* with an accuracy better than 5 μm and 10 μm respectively. A 3000-Å Al layer was applied at the water/window interface to serve as a reflector for the point-VISAR diagnostic.[13] Visual inspection (via a microscope) of the samples before they were mounted inside the anode revealed in some cases the presence of very small "bubbles," likely air. This fortuitous and normally undesirable occurrence is relevant for fully understanding the experimental results (see below).

A typical experiment consisted of applying a smooth, magnetically driven pressure ramp with a duration of about 300 ns and approximately 20 GPa maximum to the target containing the water sample. This results in the quasi-isentropic compression of water to pressures ranging from $\simeq$10 to $\simeq$16 GPa, depending on the window material. The details of the magnetic pulse generation are similar with the ones described in Ref. 12. We measured the time-dependent velocity of the interface between the water and the transpar-

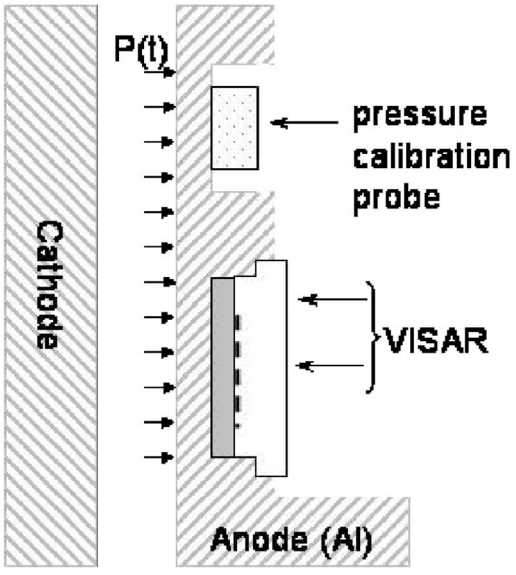

FIG. 1. Schematic cross section through target assembly. Water sample (light gray) is contained between the Al anode and the transparent window (SiO_2 or PMMA). A 3-mm vacuum gap (AK gap) separates the anode and cathode. A rapidly varying magnetic field in the AK gap generates the pressure pulse that compresses the water sample. A reference probe assembly consisting of a transparent window (LiF) impedance matched and bonded to the anode provides a direct measurement of the loading pressure profile for each sample, $P(t)$.

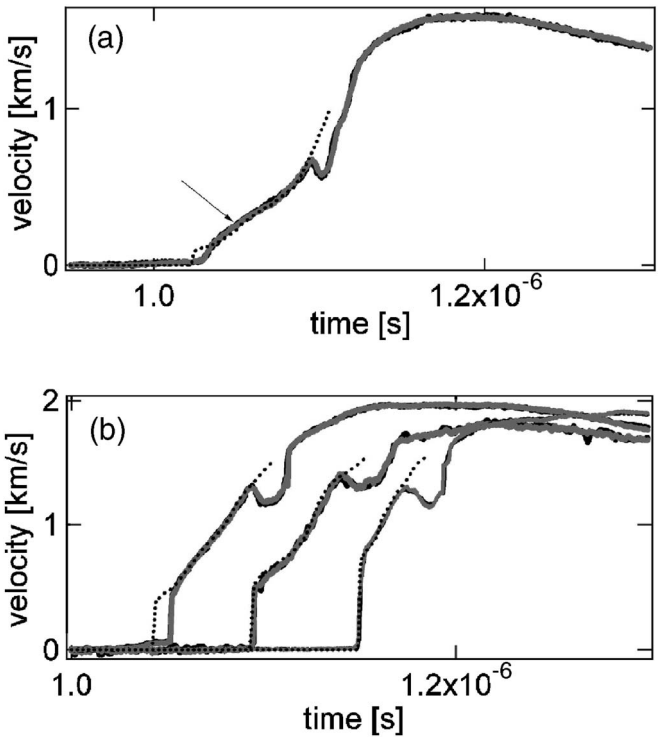

FIG. 2. VISAR traces (interface velocity) for the SiO_2 (a) and PMMA (b) windows. Solid gray and black lines: experiments. Dashed lines: single-phase hydrodynamic simulations. The arrow indicates the position of the expected, equilibrium liquid-water–ice phase transition.

ent window using a point-VISAR diagnostic. The loading pressure was also measured in all experiments using reference probes placed on each individual panel, as shown in Fig. 1. The windows used in the experiment were PMMA and fused silica (SiO_2), chosen to provide a wide range of loading conditions at the interface and in the bulk of the material (water). As discussed in Ref. 14 the dynamic impedance of the window plays an important role in the evolution of the phase transformation in the sample. The PMMA windows (density $\rho=1.186$ g/cm^3) are closely dynamically matched to water, providing a nearly *in situ* response. The silica windows, on the other hand, are denser, leading to a substantial pressure enhancement at the interface. Final pressures generated in the water are also larger, $\simeq$16 GPa, than in the case of the PMMA window.

The water/window interface velocity histories recorded during compression—$v(t)$—exhibit a smooth, gradual increase, followed by a relaxation regime with local velocity maxima at $\simeq$0.68 km/s (SiO_2) and 1.3 km/s (PMMA); see Fig. 2. In this domain the acceleration (dv/dt) appears to decrease and even change sign, signaling significant changes in the driving forces at the interface. This is followed by local minima and a resumption of velocity increases. Similar to other systems studied using dynamic compression experiments,[14] this complex behavior is related to the occurrence of a phase transformation in water at these conditions. The signature of the transformation is observed for all windows, and its onset can be identified by the change in the curvature of the $v(t)$ profiles preceding the relaxation regime. The completion of the transformation is likely marked by the ensuing velocity jump.

The nature of these observed features can be further understood by comparing the experimental results with (one-dimensional) hydrodynamic simulations. We performed such simulations using a geometry mimicking the experimental setup and employing Mie-Gruneisen equations of state for the Al anode, transparent windows, and liquid water.[15] The experimentally measured loading pressure was used for all calculations. To reproduce the initial small shocks observed in the experimental traces, which we attribute to the aforementioned "bubbles," we introduce initial "voids" in the sample with a length scale of 2%–5% of its thickness. The results of these simulations (see Fig. 2) reproduce very well the compression of liquid water even for velocities significantly higher than the ones where the equilibrium freezing transition is expected to occur—e.g., indicated by an arrow in Fig. 2(a) (SiO_2 window). This indicates that due to the rapid pressure increase, liquid water is compressed along a metastable single-phase path well beyond the liquid-solid coexistence line[16]—i.e., overcompressed. The eventual onset of freezing leads to a departure of the experimental path from the simulated one and a behavior reminiscent of a van der Waals loop,[17] connecting across the coexistence region the system responses to compression in two different phases, liquid water and crystalline ice, very likely ice VII. As opposed to an equilibrium van der Waals loop, the present loop is a complex kinetic feature due to the interplay of compression and phase transformation, which can be in principle analyzed in the context of coupled kinetics and hydrodynamics.[14] Nevertheless, the experimentally observed deceleration regime ($dv/dt<0$) can be formally attributed to the negative compressibility of the system "constrained" to a single phase, just as in the classical, equilibrium case. We therefore call this feature a kinetic van der Waals loop.

The single-phase hydrodynamic simulations allow estimates of the maximum pressures at the water/window interface ($\simeq$6–7 GPa), corresponding to isentropically overcompressed, metastable liquid water. For different experiments using the same window (PMMA) these pressures depend on the magnitude of the initial shock present in the sample. This is not unexpected since a slightly different initial shock condition places the water on neighboring, but different isentropes. The estimated overcompression of liquid water is quite significant in all experiments and appears to correspond in all cases to a liquid density of $\simeq$1.6 g/cm^3. Under equilibrium conditions the water-ice coexistence pressure for the experimental isentropes is approximately $P_c=3$ GPa.[18] Surprisingly, this corresponds to an ice density only slightly larger than $\simeq$1.6 g/cm^3. The density of ice VII at the higher pressures of 6–7 GPa is of course somewhat higher, $\sim$1.7 g/cm^3.[19] Nevertheless, these observations suggest that the freezing of water in the present experiments is rather close to a two-step process: compression close to the ice density, followed by wholesale molecular ordering—i.e., crystallization. We reached these rather extreme thermodynamic states of metastable liquid water using very high compression rates, $\simeq 10^8$ GPa/s. We estimate the temperatures corresponding to the maximum overcompressions to be $\approx$500 K. Reaching the same states through isobaric cooling

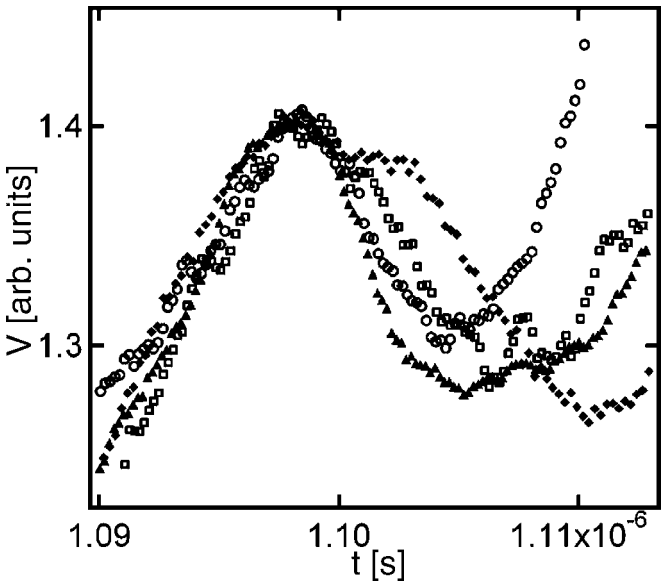

FIG. 3. Velocity relaxation regimes for all experiments, shifted and scaled to a common maximum.

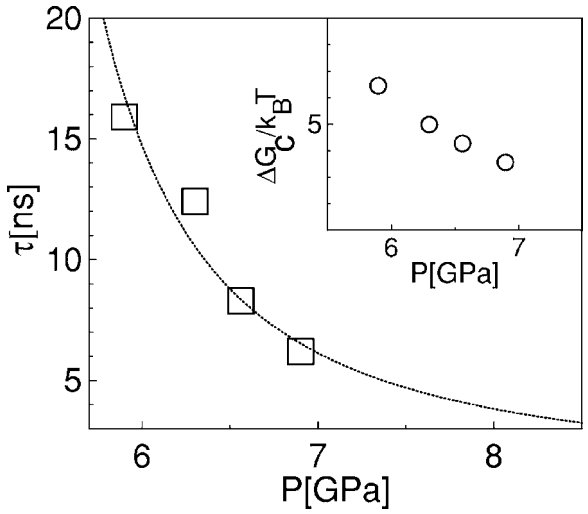

FIG. 4. Characteristic kinetic time scales as a function of pressure (see text). Inset: estimated nucleation barrier as a function of pressure.

would constitute a rather deep temperature quench and, if similar time scales were required, would involve cooling rates of roughly 10^9 K/s.

We now proceed to quantify the above observations in the framework of classical nucleation and growth theory. As pointed out in Ref. 14, when phase transformations occur under dynamic conditions the relaxation of the velocity profile is related to the characteristic time τ of the transition kinetics. For the present analysis we define these times by strict reference to the experimental traces, as the intervals between the first inflection point of the interface velocity (maximum positive acceleration) and its second inflection point following the peak (maximum negative acceleration); we show in Fig. 3 the relevant portion of the experimental traces. On comparing with the one-phase hydrodynamic simulations we also associate with the extracted times pressures corresponding to the metastable, single-phase maximum compression of liquid water above the two-phase coexistence line. Figure 4 shows the dependence of the characteristic times on these pressures for the four experiments performed, which suggests that τ is a monotonically decreasing function of pressure.

To understand this behavior we recall the well-known Kolmogorov-Johnson-Mehl-Avrami (KJMA) model of nucleation and growth.[20–22] In this framework the kinetic time scale τ contains contributions from the nucleation rate γ and the growth (interface) velocity v. For homogeneous nucleation, which we assume to be the dominant mechanism due to the large overcompressions involved, $\tau \propto (\gamma v^3)^{-1/4}$.[22] Both γ and v are in principle functions of pressure as well as temperature. According to classical nucleation theory[23] the nucleation rate γ is proportional to the probability of spontaneously overcoming a free energy barrier ΔG_c, $\gamma \propto \exp(-\Delta G_c/k_B T)$, associated with the formation of a critical-nucleus—solid (ice) crystallite. The standard analysis of bulk and surface free energy contributions associated with this process yields $\Delta G_c \propto \Delta\mu^{-2}$, where $\Delta\mu$ is the difference between the chemical potentials of the two phases, liquid and solid. Hamaya *et al.*[24] have concluded that for small metastability the interface velocity satisfies $v \propto \Delta\mu$. Upon assuming $\Delta\mu \propto \Delta P$ they therefore proposed that under isothermal conditions the characteristic time can be written as

$$\tau = A(\Delta P)^{-3/4} \exp[B(\Delta P)^{-2}], \tag{1}$$

where ΔP is the overcompression, $\Delta P = P - P_c$, with P_c the equilibrium coexistence pressure. In the present experiments the phase transformation occurs under quasiadiabatic not isothermal conditions, but the estimated temperature variation in the metastable water is rather small ($\simeq$50 K), and we expect its effect on the kinetics to be also small relative to the effect of the observed large overcompressions. We employ therefore the same functional form (1) to fit the characteristic times shown in Fig. 4. This simple exercise allows a direct estimate of the nucleation barrier ΔG_c, since $\Delta G_c/k_B T = 4B(\Delta P)^{-2}$; we show the results in the inset of Fig. 4.

Upon compression the ice nucleation barrier decreases, becoming at the highest pressures a small multiple of $k_B T$. Of course in such a regime the concept of a thermodynamic barrier starts losing much of its meaning since normal thermal fluctuations can easily overcome it. In fact, we also estimate that the critical nucleus size drops at these conditions below approximately ten molecules, which challenges the notion of a minimum size (critical) crystallite. These observations suggest that in our experiments liquid water has been overcompressed close to its thermodynamic stability boundary. Beyond this limit single-phase liquid water is thermodynamically unstable and freezing should proceed through spinodal crystallization—i.e., a collective process qualitatively different than the appearance and growth of localized nuclei typical of nucleation. It may be interesting to study this transition using molecular dynamics simulations with realistic water potentials, as recently done for the Lennard-Jones fluid.[25]

In conclusion we report high-pressure dynamic compression experiments of liquid water along a quasiadiabatic path leading to the ice-VII region of the water phase diagram. The coupling of rapidly applied pressures and phase transformation kinetics leads to the occurrence of experimental features resembling van der Waals loops. We find that metastable liquid water is compacted close to the ice density before the onset of crystallization, consistent with a two-step freezing process that involves significant disruption of the hydrogen-bonding network before freezing.[1,26] On analyzing the characteristic kinetic time scales involved we estimate the nucleation barriers and conclude that liquid water has been compressed to a high-pressure thermodynamic state close to its thermodynamic stability limit. Such a state would likely be difficult to attain through traditional isobaric temperature quenches due to the large cooling rates required.

We thank the technical staff at the Sandia Z-accelerator for assistance in executing these experiments. This work was performed under the auspices of the U.S. Department of Energy by University of California Lawrence Livermore National Laboratory under Contract No. W-7405-Eng-48.

*Electronic address: bastea1@llnl.gov

[1] M. Matsumoto, S. Saito, and I. Ohmine, Nature (London) **416**, 409 (2002).
[2] G. R. Wood and A. G. Walton, J. Appl. Phys. **41**, 3027 (1970).
[3] D. J. Safarik and C. B. Mullins, J. Chem. Phys. **121**, 6003 (2004).
[4] R. A. Shaw, A. J. Durant, and Y. Mi, J. Phys. Chem. B **109**, 9865 (2005).
[5] See, e.g., M. Song, H. Yamawaki, H. Fujihisa, M. Sakashita, and K. Aoki, Phys. Rev. B **68**, 024108 (2003) and references therein.
[6] J. D. Jorgensen and T. G. Worlton, J. Chem. Phys. **83**, 329 (1985).
[7] S. Klotz, J. M. Besson, G. Hamel, R. J. Nelmes, J. S. Loveday, and W. G. Marshall, Nature (London) **398**, 681 (1999).
[8] M. R. Frank, C. E. Runge, H. P. Scott, S. J. Maglio, J. Olson, V. B. Prakapenka, and G. Shen, Phys. Earth Planet. Inter. **155**, 152 (2006).
[9] J.-L. Kuo and M. L. Klein, J. Phys. Chem. B **108**, 19634 (2004).
[10] S. J. Singer, J.-L. Kuo, T. K. Hirsch, C. Knight, L. Ojamäe, and M. L. Klein, Phys. Rev. Lett. **94**, 135701 (2005).
[11] S. Klotz, Th. Strässle, C. G. Salzmann, J. Philippe, and S. F. Parker, Europhys. Lett. **72**, 576 (2005).
[12] C. A. Hall, J. R. Asay, M. D. Knudson, W. A. Stygar, R. B. Spielman, T. D. Pointon, D. B. Reisman, A. Toor, and R. C. Cauble, Rev. Sci. Instrum. **72**, 3587 (2001).
[13] W. F. Hemsing, Rev. Sci. Instrum. **50**, 73 (1979); L. M. Barker, in *Shock Compression of Condensed Matter–1997*, edited by S. C. Schmidt, D. P. Dandekar, and J. W. Forbes, AIP Conf. Proc. No. 429 (AIP, Woodbury, NY, 1998), pp. 833–836.
[14] M. Bastea, S. Bastea, J. A. Emig, P. T. Springer, and D. B. Reisman, Phys. Rev. B **71**, 180101 (2005).
[15] J. E. Reaugh (unpublished); S. P. Marsh, *LASL Shock Hugoniot Data* (University of California Press, Berkeley, 1980); A. C. Mitchell and W. J. Nellis, J. Chem. Phys. **76**, 6273 (1982); L. Barker and R. Hollenbach, J. Appl. Phys. **43**, 4669 (1972).
[16] F. Datchi, P. Loubeyre, and R. LeToullec, Phys. Rev. B **61**, 6535 (2000).
[17] See, e.g.., M. E. Fisher and S. Zinn, J. Phys. A **31**, 629 (1998) and references therein.
[18] D. H. Dolan, J. N. Johnson, and Y. M. Gupta, J. Chem. Phys. **123**, 064702 (2005) and references therein.
[19] Y. Fei, H.-K. Mao, and R. J. Hemley, J. Chem. Phys. **99**, 5369 (1993).
[20] A. N. Kolmogorov, Bull. Acad. Sci. USSR, Phys. Ser. (Engl. Transl.) **3**, 555 (1937).
[21] W. A. Johnson and R. F. Mehl, Trans. Am. Inst. Min., Metall. Pet. Eng. **135**, 416 (1939).
[22] M. Avrami, J. Chem. Phys. **7**, 1103 (1939); **8**, 212 (1940); **9**, 177 (1941).
[23] See, e.g., L. D. Landau and E. M. Lifshitz, *Physical Kinetics* (Butterworths-Heinemann, Oxford, 1995).
[24] N. Hamaya, Y. Yamada, J. D. Axe, D. P. Belanger, and S. M. Shapiro, Phys. Rev. B **33**, 7770 (1986).
[25] F. Trudu, D. Donadio, and M. Parrinello, Phys. Rev. Lett. **97**, 105701 (2006).
[26] A. Sanz, M. Jiménez-Ruiz, A. Nogales, D. Martín y Marero, and T. A. Ezquerra, Phys. Rev. Lett. **93**, 015503 (2004).